Electron spin resonance and relaxation studies of double-layered manganites

F. Simon,[1,2] V. A. Atsarkin,[3] V. V. Demidov,[3] R. Gáal,[1] Y. Moritomo,[4] M. Miljak,[5] A. Jánossy,[2] and L. Forró[1]
[1]*IPMC, École Polytechnique Fédérale de Lausanne, CH-1015 Lausanne, Switzerland*
[2]*Institute of Physics, Budapest University of Technology and Economics, H-1521 Budapest, P.O. Box 91, Hungary*
[3]*Institute of Radio Engineering and Electronics, Russian Academy of Sciences, 125009 Moscow, Russia*
[4]*Center for Integrated Research in Science and Engineering, Nagoya University, Nagoya 464-8601, Japan*
[5]*University of Zagreb, Institute of Physics, CR-41001 Zagreb, Croatia*
(Received 19 December 2002; published 27 June 2003)

Electronic properties of $La_{2-2x}Sr_{1+2x}Mn_2O_7$ ($x=0.4$ and 0.5) single crystals are studied by electron spin resonance (ESR) and spin-lattice relaxation time measurements. Spin susceptibility $\chi(T)$ determined from the ESR signal intensity and macroscopically measured static-susceptibility data are in good agreement, thus ESR detects all spin species in the system. In both compounds, the ESR spectra contain a single, nearly isotropic Lorentzian line associated with the exchange coupled Mn^{3+} and Mn^{4+} ions. For the $x=0.5$ compound, the fingerprints of charge ordering (CO) transition at $T_{CO}=226$ K are detected. In addition, strongly anisotropic ferromagnetic resonance spectra are found in both materials, suggesting the presence of extrinsic ferromagnetic phases. For $x=0.4$, the longitudinal relaxation time T_1 and the transversal relaxation time T_2 are equal around room temperature that is a sign of exchange narrowing. The T_1/T_2 ratio increases to about 5 approaching the Curie temperature $T_C=126$ K. No sign of critical speeding up of T_1 is detected. Instead, the slowing down of the relaxation rate takes place and T_1 is proportional to $T\chi(T)$. This is attributed to the freezing of short-range magnetic correlations in the external field.

DOI: 10.1103/PhysRevB.67.224433 PACS number(s): 76.30.−v, 76.50.+g, 75.40.−s, 75.47.−m

I. INTRODUCTION

Recently, double layered variants of the perovskite-structure manganites represented by the formula $La_{2-2x}Sr_{1+2x}Mn_2O_7$ attracted much attention due to their unusual conducting and magnetic properties, including colossal magnetoresistance (CMR), charge and orbital ordering, and especially the effects of low dimensionality (see, for example, Refs. 1–6). These crystals consist of MnO_2 bilayers separated by insulating $(La,Sr)_2O_2$ sheets, a quasi-two-dimensional (2D) structure leading to anisotropic properties. The rich phase diagram of the double layered manganites[3] shows that considerable changes in magnetic ordering can be caused by slight variations of the Mn^{4+} (i.e., hole) concentration represented by doping x. Electron spin resonance (ESR) is an important technique to study magnetically correlated materials and thus the different parts of the phase diagram of manganites. Up to now, the ESR data on the $La_{1.35}Sr_{1.65}Mn_2O_7$ ceramics[7] and $La_{1.4}Sr_{1.6}Mn_2O_7$ single crystals[8,9] were reported, both compounds revealing typical CMR behavior near the transition from paramagnetic insulator to ferromagnetic metal. Chauvet *et al.*[7] detected the presence of ferromagnetic clusters and magnetic polarons; however, some later investigations carried out on single crystals[8–10] cast doubt on this suggestion. Instead, an additional strongly anisotropic spectrum observed in most of the samples was associated with intergrowths of other perovskite phases. The relative size of the additional signal was found to depend on crystal growing conditions,[9] as would be expected from inclusions.

In this paper, we report ESR results on single crystals of $La_{1.2}Sr_{1.8}Mn_2O_7$ ($x=0.4$) and $LaSr_2Mn_2O_7$ ($x=0.5$) compounds. The $x=0.4$ material is a ferromagnetic metal (FM) below $T_C=126$ K. The half-doped $LaSr_2Mn_2O_7$ compound separates the FM and antiferromagnetic insulating (AFI) ground states and has some peculiarities: it contains equal numbers of Mn^{3+} and Mn^{4+} ions and undergoes charge ($T_{CO}=226$ K) and antiferromagnetic (AFM, $T_N=170$ K) ordering.[4] This material has not been studied by ESR to the present day.

We also studied T_1 and T_2, the longitudinal and transverse electron spin relaxation times, respectively. The relaxation rates T_1^{-1} and T_2^{-1} are proportional to the corresponding spectral densities of the internal field fluctuations,[11] and so provide a great deal of useful information about changes related to phase transitions; in particular, critical ''speeding up'' of the relaxation rates is usually expected when going through the critical temperature from above. Using conventional ESR it is impossible to measure T_1 in systems with so fast relaxation that encountered in manganites. However, the modulation technique with longitudinal detection which was originally proposed by Hérve and Pescia[12,13] and modified a few years ago[14] enables the measure of T_1 values as short as 10^{-10} s. Using this technique, T_1 have been measured[15,16] in a series of perovskite manganites $La_{1-x}Ca_xMnO_3$ in the paramagnetic state and across the Curie temperature (T_C). Striking absence of the critical speeding up of the longitudinal spin relaxation near T_C was reported, in contrast with theoretical predictions.[17–19] The origin of this phenomenon was not cleared up, and new investigation on the layered (quasi-2D) manganites is desirable. The goal of this study is to investigate spin dynamics and phase transitions in single crystals of two double layered manganites using ESR and spin relaxation techniques, with particular emphasis on critical behavior of spin relaxation and seeking for signs of magnetic polarons.

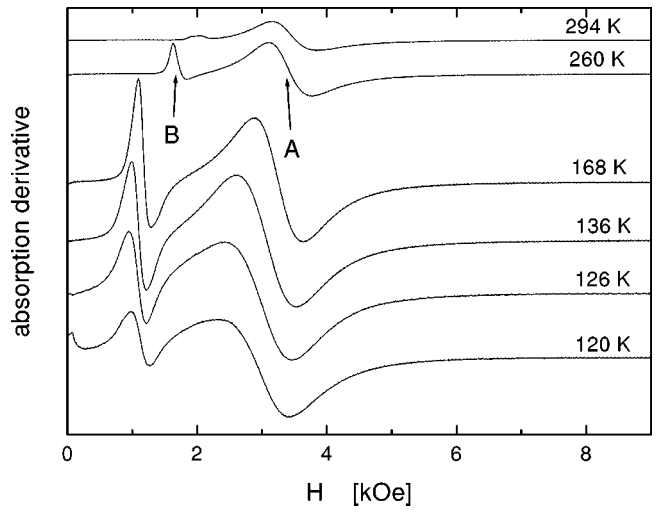

FIG. 1. Typical ESR spectra of the $La_{1.2}Sr_{1.8}Mn_2O_7$ single crystal at 9.5 GHz for **H** in the (a,b) plane. Temperatures are indicated at the curves. The arrows show the "*A*" and "*B*" lines.

II. EXPERIMENTAL TECHNIQUES

Our ESR, relaxation, and dc magnetization measurements have been carried out on single crystals of $La_{1.2}Sr_{1.8}Mn_2O_7$ ($x=0.4$) and $LaSr_2Mn_2O_7$ ($x=0.5$). The samples were platelike in shape, of a few mm^2 in area and 0.7–0.9 mm thick. The *c* axis was perpendicular to the largest plane. The crystals were prepared in the Center for Integrated Research in Science and Engineering, Nagoya University using the floating zone method. X-ray characterization showed that the crystals were of high quality. The ESR spectra at 9.5 GHz (*X* band) were taken in Bruker ESR spectrometers in Moscow and Lausanne; the high-frequency measurements (at 75 and 150 GHz) were performed in Budapest in a home-built spectrometer. The dc magnetization studies were carried out in Zagreb with a torque magnetometer. The longitudinal electron spin relaxation time T_1 was measured by the modulation technique previously described in Refs. 12–16. The method involves detection of the longitudinal magnetization response to radio-frequency modulation of the microwave power acting upon the ESR line. The "amplitude" version[14–16] was used, which is in fact analogous to the conventional cw saturation technique, with the difference that the extremely low saturation factors ($s\sim10^{-3}-10^{-4}$) are employed; they are measured by means of the longitudinal detection. The modulation frequency of 1.6 MHz and microwave power (in the *X* band) of about 200 mW were used. We employed diphenyl-picryl-hydrazyl (DPPH) as a standard reference with temperature-independent value of $T_1=5\times10^{-8}$ s.

III. RESULTS

A. ESR spectra and susceptibilities

Typical ESR spectra of $La_{1.2}Sr_{1.8}Mn_2O_7$ ($x=0.4$) and $LaSr_2Mn_2O_7$ ($x=0.5$) taken in the *X* band at various temperatures are presented in Figs. 1, 2(a), and 2(b). In both compounds, above critical temperatures, the spectra include

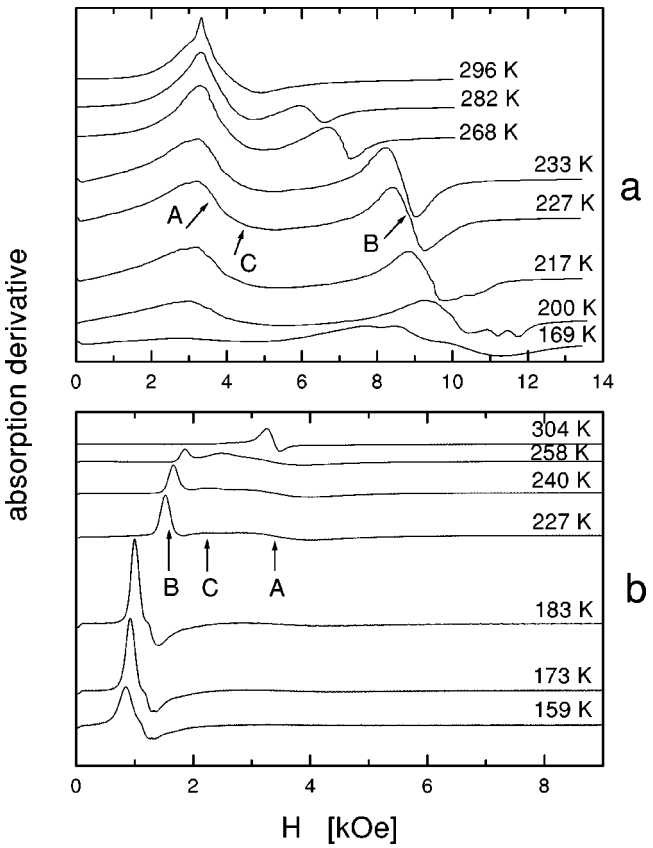

FIG. 2. Typical ESR spectra taken on the $LaSr_2Mn_2O_7$ single crystal at 9.5 GHz; (a) $\mathbf{H}\|c$; (b) **H** in the (a,b) plane. Temperatures are indicated at the curves. The "*A*," "*B*," and "*C*" lines are shown by the arrows.

a broad, slightly anisotropic line (called the "*A* line") characterized by a *g* factor close to 2, and strongly anisotropic line "*B*." In addition, a weak additional line (called the "*C* line") is observed in $LaSr_2Mn_2O_7$; this line is not well resolved in the ESR spectra (see Fig. 2), but it is clearly seen in the longitudinal response due to its relatively large T_1 value (see below, Sec. III B). All the lines are shifted from their high-temperature position ($g\approx2$) to higher fields when the external magnetic field **H** is along the *c* axis, and to lower ones when **H** is in the (a,b) plane. The spectra of $La_{1.2}Sr_{1.8}Mn_2O_7$ are similar to those reported previously.[8,9] The resonance fields H_A, H_B, and H_C of the corresponding lines for the $x=0.5$ compound (after corrections made for the Dysonian distortion, see below) are plotted in Fig. 3 versus temperature. The temperature interval in Fig. 3 is restricted to the range where the resolution allows determination of the resonance fields with proper accuracy.

The behavior of the *A* line can be attributed to ordinary paramagnetic resonance of the exchange coupled $Mn^{3+}-Mn^{4+}$ spin system. For $x=0.4$, this was thoroughly discussed in previous publications.[8,9] As clearly demonstrated by Moreno *et al.*,[9] the shifts of the *A* line to higher and lower fields are proportional to magnetization (*M*) of the paramagnetic sample and can be associated with the single-ion anisotropy and Dzialoshinsky-Moriya interaction. In the $x=0.5$ compound, the H_A value depends on *T* only slightly

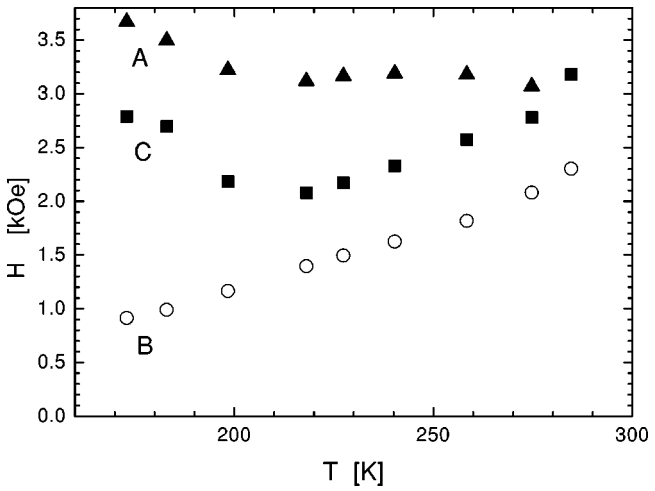

FIG. 3. The resonance fields of the *A* line (triangles), *B* line (circles), and *C* line (squares) in $LaSr_2Mn_2O_7$; **H** in the (a,b) plane.

(Fig. 3), in agreement with expected low magnetization values typical of AFM materials. Note that both H_A and H_C temperature dependencies change their slopes below $T_{CO} \simeq 220$ K.

As to the strongly anisotropic *B* line, there are some discrepancies in the interpretation of its origin. In the early work by Chauvet *et al.*[7] (performed on ceramics with $x = 0.325$), this line was attributed to intralayer ferromagnetic clusters of fixed (microscopic) size. Instead, in more recent publications,[8,9] the *B* line observed in the $x = 0.4$ single crystals was considered as ferromagnetic resonance (FMR) originating from intergrowths of other parasitic phases undergoing ferromagnetic transition below $T_C^* \approx 270$ K. Figure 4 shows temperature dependence of the shift $H_B - H_A$ of the *B* line relative to the nearly isotropic *A* line; the presented data are taken on the $x = 0.5$ sample at various microwave frequencies (from $\omega/2\pi = 9.5$ to 150 GHz) for both *c* and (a,b) directions of the magnetic field. The shift is nearly independent of ω and so caused by the effect of the sample magnetization rather than *g*-factor anisotropy. The dependence of H_B on the angle θ between the **H** direction and the *c* axis is shown in Fig. 5. The plot is typical of FMR in thin ferromagnetic platelet or, alternatively, of anisotropic ferromagnet with an easy plane (see below, Sec. IV).

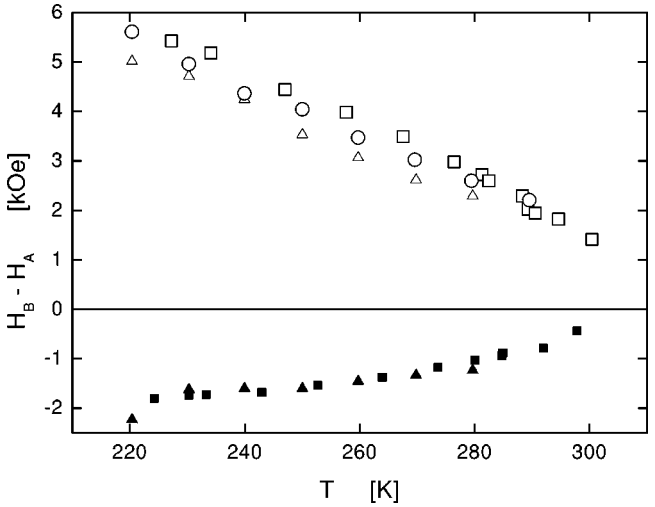

FIG. 4. Shift of the resonance field of the *B* line in $LaSr_2Mn_2O_7$ at $\mathbf{H} \| c$ (open symbols) and in the (a,b) plane (filled symbols) relative to the *A* line as a function on temperature. Squares: 9.5 GHz; triangles: 75 GHz; circles: 150 GHz.

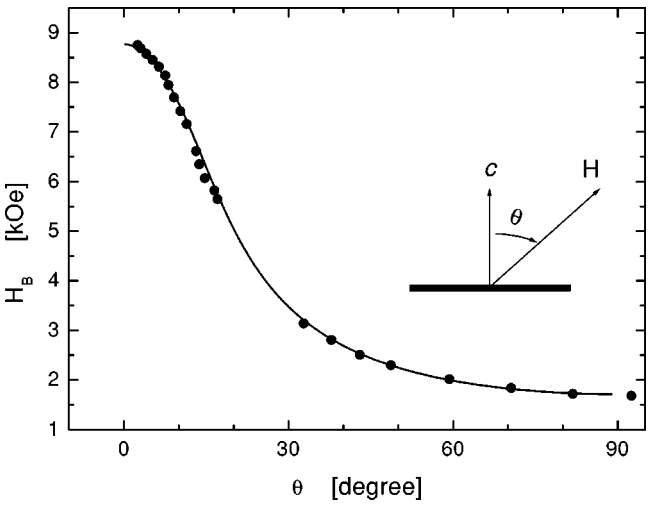

FIG. 5. Angular dependence of the resonance shift of the *B* line in $LaSr_2Mn_2O_7$ at $T = 236$ K. The solid curve is calculated from the model of an easy-plane ferromagnet with $H_{anis} = 2.65$ kOe.

The ESR lines in Figs. 1 and 2 are asymmetric. This seems to be natural due to an admixture of the dispersionlike (Dysonian) component typical of conducting samples having their skin depth δ at microwave frequencies of the order of the sample thickness (d). We have performed corresponding correction[20,21] by means of subtracting the dispersionlike (symmetric) part of the *A*-line absorption derivative. As a result, the values of d/δ presented in Fig. 6 were worked out, which are in agreement with conductivity data.[2,6,22] Once the correction has been made, the *A* line was found to be well

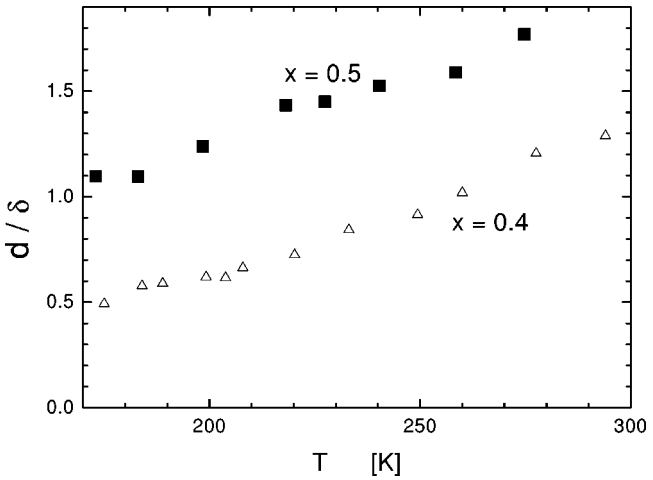

FIG. 6. Sample thickness (d) over skin depth (δ) versus temperature for $La_{1.2}Sr_{1.8}Mn_2O_7$ (open triangles) and $LaSr_2Mn_2O_7$ (filled squares).

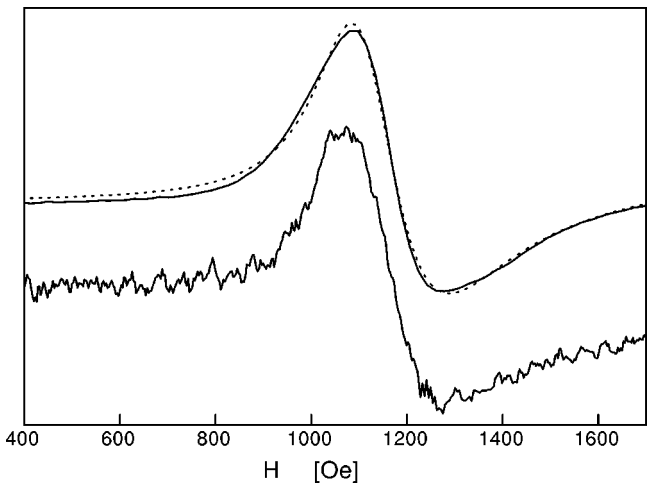

FIG. 7. The shape of the *B* line after subtracting the Dysonian distortion (at the top) and the same line recorded by longitudinal detection (below), both registered on $La_{1.2}Sr_{1.8}Mn_2O_7$ at $T=168$ K and **H** in the (a,b) plane. The dotted line represents the best fit accounting for distribution of the Lorentzian packets, see the text.

described by Lorentzian shape in the whole temperature range corresponding to paramagnetic phases of the both compounds (above $T_N=170$ K for $x=0.5$ and $T_C=126$ K for $x=0.4$). Below these critical temperatures, additional shifts and distortions arise, typical of long-range magnetic ordering.

Using the determined d/δ ratios, we performed similar correction for the *B* line. It was found, however, that the *B* line is strongly asymmetric in both compounds even after subtraction of the Dysonian distortion. This suggests inhomogeneous broadening caused by random deflection of ferromagnetic magnetization from the (a,b) plane.

To check the validity of the correction procedure, the ESR spectra obtained after subtracting the Dysonian distortion were compared with those observed by means of the longitudinal detection used for T_1 measuring (see below). It should be noted that the longitudinal magnetization response is proportional to the absorbed microwave power. So it is insensitive to the ''dispersion'' mode and presents the pure absorption spectrum. It was found that both methods of registering the resonance absorption spectra are in good agreement. An example is shown in Fig. 7.

Knowing the corrected absorption spectra and the skin depth values, the total resonance absorption areas of each ESR line can be used to determine χ_A, χ_B, and χ_C, the ESR susceptibilities related to the *A*, *B*, and *C* lines. The corresponding temperature dependencies are shown in Figs. 8 and 9. The overall temperature dependence of the macroscopic static susceptibility $\chi_0(T)$, determined on the $x=0.5$ sample from the torque measurements agrees with the sum of the ESR susceptibilities $\chi_{ESR}=\chi_A+\chi_B+\chi_C$. Moreover, the maximum absolute values, $\chi_0(226\text{ K})=2.3\times10^{-4}$ emu/g and $\chi_{ESR}(226\text{ K})=3\times10^{-4}$ emu/g, are within 30%. Such an agreement is usually considered as a strong evidence that all spin species are accounted for in the ESR experiment.

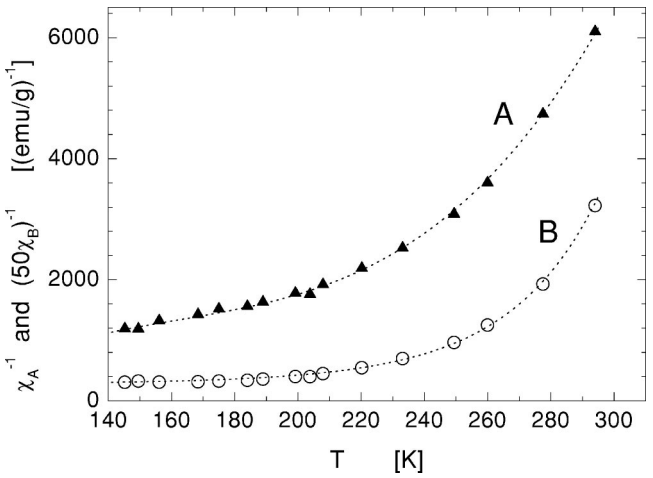

FIG. 8. Temperature dependencies of the inverse ESR susceptibility of the *A* line (filled triangles) and the *B* line (open circles; note the scale change) for $La_{1.2}Sr_{1.8}Mn_2O_7$; **H** in the (a,b) plane. Dashed lines are guides for the eyes.

We observed that $\chi_A(T)$ deviates from the Curie-Weiss behavior in the $x=0.4$ sample, thus pointing to the existence of superparamagnetic clusters (short-range ferromagnetic correlations). Unlike this, for the $x=0.5$ material both χ_A and χ_C pass through maxima in the vicinity of $T_{CO}=226$ K, the temperature of the charge ordering. As to χ_B, saturation of the magnetization is clearly seen in both compounds, that confirms the ferromagnetic nature of the *B* line.

B. Relaxation

Temperature dependencies of T_1 and T_2 for the $x=0.4$ crystal are shown in Fig. 10 with T_2 values calculated from the equation

$$T_2^{-1}=\gamma\Delta_L\,. \tag{1}$$

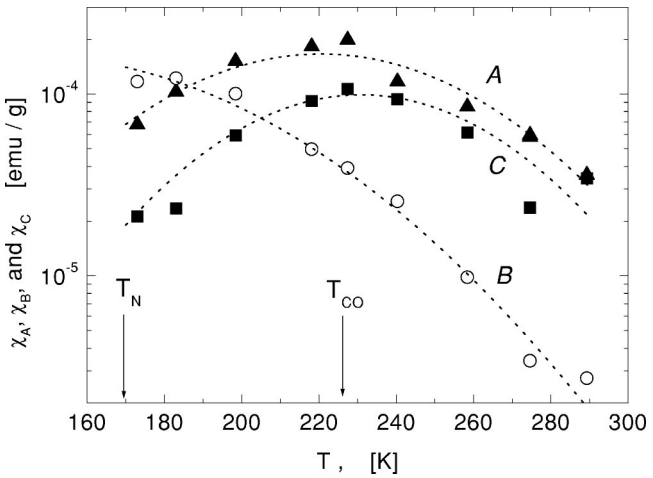

FIG. 9. Temperature dependencies of partial ESR susceptibilities (*A* line: filled triangles; *B* line: open circles; *C* line: filled squares) for $LaSr_2Mn_2O_7$; **H** in the (a,b) plane. Dashed lines are guides for the eyes.

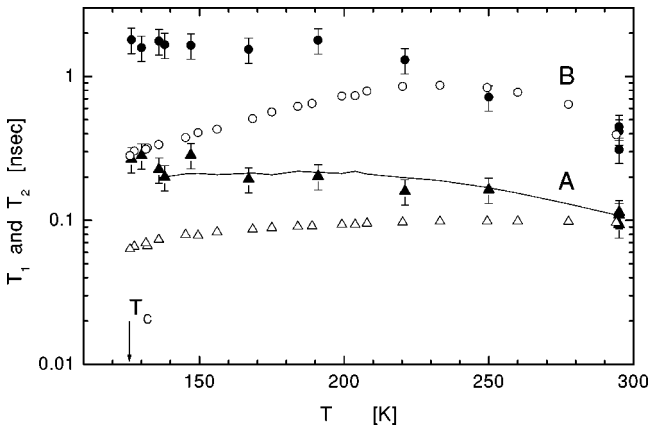

FIG. 10. Temperature dependencies of the longitudinal (T_1, solid symbols) and transverse (T_2, open symbols) relaxation times for $La_{1.2}Sr_{1.8}Mn_2O_7$; **H** in the (a,b) plane. Triangles: *A* line; circles: *B* line. Solid curve represents the ''noncritical Huber law,'' Eq. (2).

Here $\gamma = g\mu_B/\hbar$ is the electron spin magnetogyric ratio (μ_B being the Bohr magneton and $\hbar$ the Planck constant), and Δ_L is the half-width of the Lorentzian *A* line or a spin packet forming the inhomogeneous *B* line (see below, Sec. IV). One can see in Fig. 10 that the $T_1 = T_2$ equality holds for the *A* and *B* lines only at the highest part of the temperature range. Upon cooling below 250–300 K, the T_1/T_2 ratio increases progressively to about 5 when approaching the Curie temperature. Moreover, the temperature dependence of T_1 for the *A* line can be well fitted by the ''non-critical Huber law'' [23] (see below, Sec. IV),

$$T_1 \propto T\chi(T), \tag{2}$$

where the temperature dependent susceptibility $\chi(T)$ was taken from Fig. 8. In Fig. 10, the relation Eq. (2) is represented by the solid curve. Similar behavior was reported on the $La_{1-x}Ca_xMnO_3$ manganites[15,16] with the difference that, in the $La_{1-x}Ca_xMnO_3$ case, the ''slowing down'' of T_1 and raising of T_1/T_2 were observed only in a narrow temperature range just above the Curie point.

Relaxation data for $x = 0.5$ are presented in Fig. 11. In this case, the longitudinal response from the *A* line was too weak to be detected with proper accuracy, so only upper limit of about 0.1 ns has been determined for $T_1(A)$ (it will be recalled that the magnitude of the longitudinal response is proportional to T_1, see Ref. 14). Unlike this, the T_1 values measured on the *B* line and *C* line were found to be sufficiently long. The largest T_1/T_2 ratio is observed on the *C* line, being indicative of strong inhomogeneous broadening.

IV. DISCUSSION

First, we will discuss the origin of the ferromagnetic (*B*-line) spectra observed in both $x = 0.4$ and 0.5 compounds. The most plausible (and the simplest) model was suggested in Refs. 8–10 where the *B* line was attributed to thin ferromagnetic platelets (intergrowths) which occupy only a few percent of the total volume. The observed anisotropy was

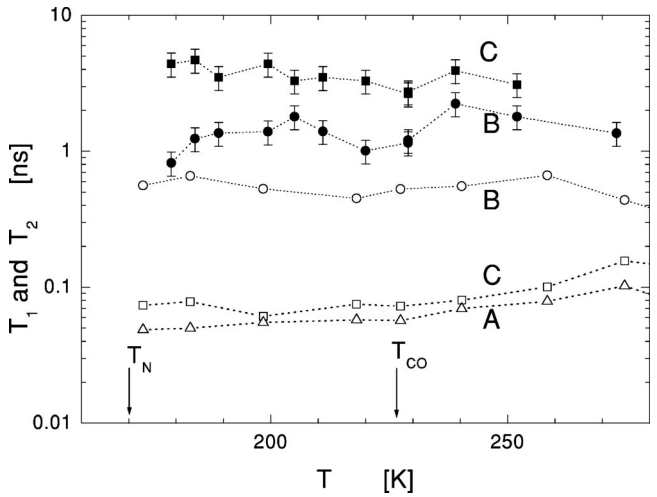

FIG. 11. Temperature dependencies of T_1 (filled symbols) and T_2 (open symbols) in the $LaSr_2Mn_2O_7$ crystal with **H** in the (a,b) plane. Triangles: *A* line; circles: *B* line; squares: *C* line. Dashed lines are guides for the eyes.

assumed to be caused by demagnetization field according to the well-known formulas[24]

$$\left(\frac{\omega}{\gamma}\right)^2 = H(H + 4\pi M), \quad \mathbf{H} \text{ in } (a,b) \text{ plane}, \tag{3a}$$

$$\frac{\omega}{\gamma} = H - 4\pi M, \quad \mathbf{H} \| c. \tag{3b}$$

In the work by Bhagat *et al.*,[8] this model was successfully used for fitting the observed angular dependence of the resonance field H_B. It should be emphasized, however, that the fitting of the same quality can be obtained with another approach, namely, by accounting for anisotropic ferromagnetism with an easy (a,b) plane that is just the case for the double layered manganites.[1–6] In this model, Eqs. 3(a) and 3(b) remain valid after substitution of anisotropy field H_{anis} for $2\pi M$ (see Ref. 24). The calculated angular dependence of H_B for $x = 0.5$ is shown in Fig. 5 together with the experimental data; the best fit was obtained at $H_{\text{anis}} = 2.65$ kOe ($x = 0.5$) and 2.2 kOe ($x = 0.4$; not shown). So the model of intralayer ferromagnetic clusters proposed by Chauvet *et al.*[7] cannot be conclusively excluded if one suggests that the cluster size is large enough to be considered as an anisotropic object allowing observation of the FMR spectrum.

Some information on this subject can be obtained from the behavior of the *B*-line parameters in the vicinity of critical points (T_C, T_{CO}, and T_N) characterizing the host lattice (and not the intergrowths) of the manganite crystals. First, as can be seen in Fig. 2, the AFM ordering below $T_N = 170$ K (at $x = 0.5$) manifest itself in the splitting of the *B* line. Secondly, there is a slight dip in the temperature dependence of the longitudinal relaxation rate near T_{CO} (Fig. 11); however, this effect might fall within the experimental error. The most pronounced peculiarity can be observed as follows.

As mentioned above, the overall asymmetric shape of the *B* line was supposed to be formed by superposition of ho-

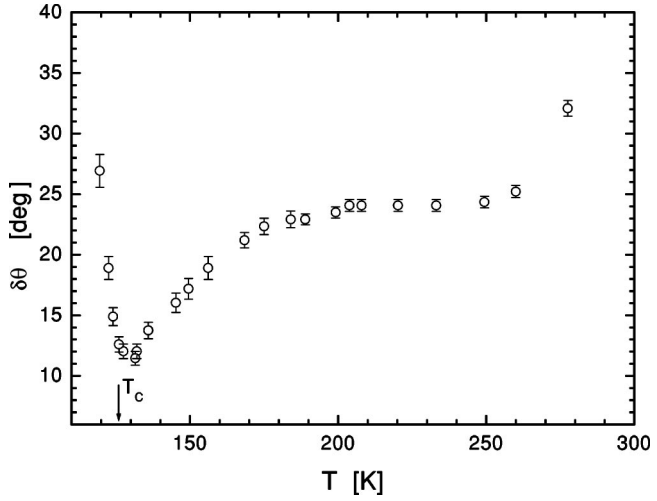

FIG. 12. The width of the angular distribution of the magnetization direction as obtained from the analysis of the *B*-line shape in $La_{1.2}Sr_{1.8}Mn_2O_7$ versus temperature; **H** in the (a,b) plane.

mogeneous Lorentzian FMR lines (spin packets) shifted by local magnetization with different values of θ, the angle between **M** and the *c* axis. Using the *M* values obtained from Eq. (3a) and assuming Gaussian distribution of θ around $\pi/2$ with the dispersion $\langle \delta\theta^2 \rangle$ as a fitting parameter, the resulting line shapes were calculated and successfully fitted to the observed ones. Temperature dependence of $\delta\theta$ for the $x=0.4$ sample is shown in Fig. 12. A pronounced minimum is clearly observed at $T_C=126$ K.

So there exist some correlation between the behavior of the ferromagnetic *B* line and the state of the surrounding background. On one hand, this might support the idea of microscopic origin of the ferromagnetic objects in question;[7] on the other hand, the FMR parameters in any thin flake of parasitic phase should be affected by the surface conditions dependent on magnetic order in the environment.

Similar arguments can be related to the *C* line observed in the $x=0.5$ sample. The anisotropy of the *C* line is intermediate between the ''normal'' paramagnetic *A* line and ferromagnetic *B* line (see Fig. 3). According to Ref. 9, the shift of the resonance field to lower values upon cooling can be caused by increasing magnetization with account made for the crystal field anisotropy. Thus the observed change in the temperature dependencies of both H_A and H_C below T_{CO} is consistent with progressive decreasing of magnetization due to development of antiferromagnetic correlations. This is supported by the susceptibility data. As it is seen from Fig. 9, the temperature dependence of χ_C is quite similar to that of χ_A: both χ_A and χ_C pass through their maxima at the charge ordering temperature T_{CO}. Thus the *C* line might be attributed either to magnetic polarons or to another parasitic phase. In fact, a borderline separating two models is rather uncertain and reduces to distinction between a microscopic spin cluster and macroscopic ferromagnetic phase. What should be the cluster size (i.e., how many exchange coupled spins should be involved) to be considered as a macroscopic ferromagnet? Whether 16 *Mn*, as suggested by Chauvet *et al.*,[7] are sufficient? Note that the existence of ~0.8 nm ferromagnetic clusters (magnetic polarons) embedded in a short-range charge/orbital matrix was reported recently for some ''cubic'' manganites.[25] Nevertheless, at the moment we cannot be sure about the origin of the *B* and *C* lines: further investigation is needed, both theoretical and experimental, to resolve this problem.

Finally, we discuss the relaxation data. The theory of electron spin relaxation in a concentrated paramagnet undergoing FM or AFM phase transition was elaborated by Kawasaki[17] and Huber;[18,19] further development and applications to ESR data were performed in a number of studies (see, e.g., Refs. 23 and 26–32). The theory is concerned with strong isotropic exchange interaction that averages an anisotropic part of spin-spin interactions (as well as the single-spin anisotropy due to the crystalline field), thus resulting in effective line narrowing. It was suggested that approaching T_C or T_N from higher temperatures results in increase of the lifetime and correlation length of critical fluctuations related with FM or AFM short-range ordering. This should lead to the critical broadening of the ESR line (''speeding up'' of the transverse spin relaxation rate $1/T_2$). The general expression describing the temperature dependence of $1/T_2$ has the form[23]

$$T_2^{-1}=\frac{C+f(\varepsilon)}{T\chi(T)}, \tag{4}$$

where *C* is a temperature independent parameter; $f(\varepsilon)$ accounts for the critical speeding up; here $\varepsilon=(T/T_c-1)$, where T_c is the critical temperature. At $T \gg T_c$, the second term in the nominator of Eq. (4) is negligible, and Eq. (4) reduces to the ''noncritical Huber law''

$$T_2^{-1}=\frac{C}{T\chi(T)}. \tag{5}$$

[This is equivalent to Eq. (2) if one accepts $T_1=T_2$ as typical of the exchange narrowed ESR spectra]. Upon heating, the noncritical relaxation rate increases for FM ordering materials and decreases for AFM ones, according to the Curie-Weiss Law; in both cases, it tends to a constant value at high temperatures. Such behavior was really observed in a number of paramagnetic substances, including the ''cubic'' $La_{1-x}Me_xMnO_3$ manganites.[33,34]

In the vicinity of the transition, the $f(\varepsilon)$ term in Eq. (4) becomes dominant and diverges as χ^α, where $\alpha>1$ is a critical exponent depending on specific mechanism of the magnetic ordering.[17–19] This critical speeding up of spin relaxation was indeed observed in several substances undergoing AFM and FM transitions,[26–29] but was not found in some others, such as yttrium and manganese ferrites,[30] yttrium-iron garnets,[31] and, what is most intriguing, in the nonlayered CMR manganites. In the latter case, the broadening of the ESR line near T_C claimed initially by many authors as the ''critical'' one, was then suggested to be inhomogeneous[35,36] and proved to be caused by the demagnetization fields in the presence of sample irregularities.[37,38] Absence of any critical speeding up and, on the contrary, the critical slowing down of the longitudinal relaxation rate (T_1^{-1}) which

obeys the relation of Eq. (2), was observed recently on the $La_{1-x}Ca_xMnO_3$ ($x=0.1-0.33$) materials by Atsarkin *et al.*[15,16]

Consider now the temperature dependencies of both T_2 and T_1 for our $x=0.4$ crystal (Fig. 10). One can see that the T_2 value determined from the *A* linewidth shortens as temperature approaches T_C (Fig. 10). This was interpreted by Moreno *et al.*[9] as Huber's critical speeding up. However, the longitudinal relaxation time of the *A* line does not demonstrate any acceleration upon cooling; instead, it increases progressively in a good agreement with Eq. (2) as represented by the solid curve in Fig. 10. So the conclusion[9] about critical behavior of the ESR linewidth appears to be doubtful. Rather, an increasing contribution of inhomogeneous broadening can be suggested, which is caused by random static fields of the exchange coupled FM clusters polarized in the external field **H**. Similar increase of the T_1/T_2 ratio upon cooling is also observed on the *B* line ascribed to FMR. In this case, however, the Huber's formulas are not applicable. Here, we cannot discuss this issue, mainly because the origin of the *B* line is not clear. Absence of the critical speeding up was also found in the $x=0.5$ crystal, both for the *B* and *C* lines (Fig. 11). Suppression of the critical speeding up in spin relaxation may be caused by the influence of the external field *H* (see Refs. 26, 29). Corresponding theory was developed by Lazuta *et al.*,[39,40] however, detailed discussion on this subject is beyond the scope of our present work, and we shall restrict our consideration to simplified estimation. Kawasaki[17] predicted that the critical broadening of the ESR linewidth in ferromagnets is expected only in the small-field limit

$$H \ll H_{\mathrm{ex}}\left(\frac{d}{l_c}\right)^{3/2}, \tag{6}$$

where $H_{\mathrm{ex}} \sim k_B T_C / g\mu_B$ is the exchange field, d is the lattice constant, and l_c is the correlation length. In conventional paramagnetic materials, the correlation length steeply increases only in a close vicinity of T_C; in such a case, Eq. (6) is fulfilled in a broad temperature range above T_C, provided that H_{ex} is large enough. In the CMR manganites, however, strong ferromagnetic correlations develop even in the paramagnetic phase, well above T_C (see Ref. 41, and references therein). As a result, the d/l_c ratio is small, the inequality (6) breaks down, and the critical acceleration of relaxation is absent. Total suppression of the critical speeding up in the muon spin relaxation by the external field of 3 kOe was demonstrated on the $La_{1-x}Ca_xMnO_3$ manganite.[42]The essence of this effect lies in the fact that local fields produced by the polarized spin clusters become static and so lead to the inhomogeneous broadening of the ESR line (apparently increasing $1/T_2$), whereas $1/T_1$, being insensitive to static fields, remains unaffected. In the layered manganites studied in the present work, the correlation lengths at $T>T_C$, T_N are expected to be even larger because of quasi-2D dimensionality. As a result, the T_1/T_2 ratio exceeds unity at much higher temperatures such as $\varepsilon \sim 2$, see Fig. 10.

The absence of critical speeding up in the CMR manganites might also be caused by the existence of strong AFM correlations which, on the one hand, are typical of these materials,[2,5,41] and on the other can suppress the ''Huber decay'' in the vicinity of the transition temperature.[43,30]

In conclusion, a comparison study of ESR, susceptibility, and longitudinal spin relaxation have been performed on two $La_{2-2x}Sr_{1+2x}Mn_2O_7$ double layered manganites differing in their magnetic ordering. From temperature dependencies of the ESR susceptibilities, definite evidences are found for ferromagnetic ($x=0.4$) and antiferromagnetic ($x=0.5$) correlations well above the magnetic ordering temperatures, with a pronounced peculiarity near T_{CO} for $x=0.5$. Additional strongly anisotropic FMR-like spectra were observed in both materials, suggesting FM intergrowths or large FM ordered clusters. Measurements of longitudinal spin relaxation have revealed the proportionality between T_1 and $T\chi(T)$ (the noncritical Huber law) in the whole temperature range. The absence of critical speeding up of the longitudinal spin relaxation and growing the T_1/T_2 ratio as approaching the phase transitions from the paramagnetic state were observed, analogous to the ''cubic'' perovskite manganites. This can be caused by freezing of the dynamical spin fluctuations due to partial ordering of superparamagnetic spin clusters in the external magnetic field.

ACKNOWLEDGMENTS

The research was supported by the Swiss National Science Foundation (Grant No. 7GEPJ062429), the Russian Foundation for Basic Research (Grant No. 02-02-16219), and the Hungarian State Grants No. OTKA T029150, OTKA TS040878, and FKFP 0352/1997. One of the authors (F.S.) acknowledges the HAS-Bolyai for support.

[1] Y. Moritomo, A. Asamitsu, H. Kuwahara, and Y. Tokura, Nature (London) **380**, 141 (1996).

[2] T. G. Perring, G. Aeppli, Y. Moritomo, and Y. Tokura, Phys. Rev. Lett. **78**, 3197 (1997).

[3] C. D. Ling, J. E. Millburn, J. F. Mitchell, D. N. Argyriou, J. Linton, and H. N. Bordallo, Phys. Rev. B **62**, 15096 (2000).

[4] D. N. Argyriou, H. N. Bordallo, B. J. Campbell, A. K. Cheetham, D. E. Cox, J. S. Gardner, K. Hanif, A. dos Santos, and G. F. Strouse, Phys. Rev. B **61**, 15269 (2000).

[5] D. B. Romero, Y. Moritomo, J. F. Mitchell, and H. D. Drew, Phys. Rev. B **63**, 132404 (2001).

[6] C. L. Zhang, X. J. Chen, C. C. Almasan, J. S. Gardner, and J. L. Sarrao, cond-mat/0203197 (unpublished).

[7] O. Chauvet, G. Goglio, P. Molinie, B. Corraze, and L. Brohan, Phys. Rev. Lett. **81**, 1102 (1998).

[8] S. M. Bhagat, S. E. Lofland, and J. F. Mitchell, Phys. Lett. A **259**, 326 (1999).

[9] N. O. Moreno, P. G. Pagliuso, C. Rettori, J. S. Gardner, J. L.

Sarrao, J. D. Thompson, D. L. Huber, J. F. Mitchell, J. J. Martinez, and S. B. Oseroff, Phys. Rev. B **63**, 174413 (2001).
[10] C. D. Potter, M. Swiatek, S. D. Bader, D. N. Argyriou, J. F. Mitchell, D. J. Miller, D. G. Hinks, and J. D. Jorgensen, Phys. Rev. B **57**, 72 (1998).
[11] A. Abragam, *The Principles of Nuclear Magnetism* (Clarendon Press, Oxford, 1961).
[12] J. Hérve and J. Pescia, C. R. Hebd. Seances Acad. Sci. **251**, 665 (1960).
[13] J. Pescia, Ann. Phys. (Paris) **10**, 389 (1965).
[14] V. A. Atsarkin, V. V. Demidov, and G. A. Vasneva, Phys. Rev. B **52**, 1290 (1995).
[15] V. A. Atsarkin, V. V. Demidov, G. A. Vasneva, and K. Conder, Phys. Rev. B **63**, 092405 (2001).
[16] V. A. Atsarkin, V. V. Demidov, G. A. Vasneva, and D. G. Gotovtsev, Appl. Magn. Reson. **21**, 147 (2001).
[17] K. Kawasaki, Prog. Theor. Phys. **39**, 285 (1968).
[18] D. L. Huber, J. Phys. Chem. Solids **32**, 2145 (1971).
[19] D. L. Huber, Phys. Rev. B **6**, 3180 (1972).
[20] L. Walmsley, J. Magn. Reson., Ser. A **122**, 209 (1996).
[21] H. Kodera, J. Phys. Soc. Jpn. **28**, 89 (1970).
[22] T. Kimura, R. Kumai, Y. Tokura, J. Q. Li, and Y. Matsui, Phys. Rev. B **58**, 11 081 (1998).
[23] D. L. Huber and M. S. Seehra, J. Phys. Chem. Solids **36**, 723 (1975).
[24] A. G. Gurevich, *Magnetic Resonance in Ferrites and Antiferromagnets* (Nauka, Moscow, 1973) (in Russian).
[25] J. M. De Teresa, M. R. Ibarra, P. Algarabel, L. Morellon, B. Garcia-Landa, C. Marquina, C. Ritter, A. Maignan, C. Martin, B. Raveau, A. Kurbakov, and V. Trounov, Phys. Rev. B **65**, 100403(R) (2002).
[26] M. S. Seehra and R. P. Gupta, Phys. Rev. B **9**, 197 (1974).
[27] E. Dormann and V. Jaccarino, Phys. Lett. A **48**, 81 (1974).
[28] R. H. Taylor and B. R. Coles, J. Phys. F: Met. Phys. **5**, 121 (1975).
[29] V. N. Berzhanskii, V. I. Ivanov, and A. V. Lazuta, Solid State Commun. **44**, 771 (1982).
[30] V. N. Berzhanskii and V. I. Ivanov, Phys. Status Solidi B **151**, 259 (1989).
[31] I. Laulicht, J. T. Suss, and J. Barak, J. Appl. Phys. **70**, 2251 (1991).
[32] A. G. Flores, V. Raposo, J. Iniguez, S. B. Oseroff, and C. De Francisco, J. Magn. Magn. Mater. **226–230**, 574 (2001).
[33] M. T. Causa, M. Tovar, A. Caneiro, F. Prado, D. Ibanez, C. A. Ramos, A. Butera, B. Alascio, X. Obradors, S. Pinol, F. Rivadulla, C. Vasques-Vasques, M. A. Lopez-Quintela, J. Rivas, Y. Tokura, and S. B. Oseroff, Phys. Rev. B **58**, 3233 (1998).
[34] D. L. Huber, G. Alejandro, A. Caneiro, M. T. Causa, F. Prado, M. Tovar, and S. B. Oseroff, Phys. Rev. B **60**, 12155 (1999).
[35] S. E. Lofland, P. Kim, P. Dahiroc, S. M. Bhagat, S. D. Tyagi, S. G. Karabashev, D. A. Shulyatev, A. A. Arsenov, and Y. Mukovskii, Phys. Lett. A **233**, 467 (1997).
[36] M. Dominguez, S. E. Lofland, S. M. Bhagat, A. K. Raychaudhuri, H. L. Ju, T. Venkatesan, and R. L. Greene, Solid State Commun. **97**, 193 (1996).
[37] F. Rivadulla, M. A. Lopez-Quintela, L. E. Hueso, J. Rivas, M. T. Causa, C. Ramos, R. D. Sanchez, and M. Tovar, Phys. Rev. B **60**, 11 922 (1999).
[38] F. Rivadulla, L. E. Hueso, M. A. Lopez-Quintela, J. Rivas, and M. T. Causa, Phys. Rev. B **64**, 106401 (2001).
[39] A. V. Lazuta, S. V. Maleyev, and B. P. Toperverg, Zh. Eksp. Teor. Fiz. **81**, 2095 (1981).
[40] A. V. Lazuta, S. V. Maleyev, and B. P. Toperverg, Solid State Commun. **39**, 17 (1981).
[41] E. L. Nagaev, Phys. Rep. **346**, 387 (2001).
[42] R. H. Heffner, L. P. Le, D. E. MacLaughlin, G. M. Luke, K. Kojima, B. Nachumi, Y. J. Uemura, G. J. Nieuwenhuys, and S.-W. Cheong, Physica B **230–232**, 759 (1997).
[43] S. V. Maleev, Pis'ma Zh. Eksp. Teor. Fiz. **26**, 523 (1977).